NASA Technical Memorandum 100561

MINIMUM WEIGHT DESIGN OF RECTANGULAR AND TAPERED HELICOPTER ROTOR BLADES WITH FREQUENCY CONSTRAINTS

Aditi Chattopadhyay and Joanne L. Walsh

February 1988

National Aeronautics and Space Administration

Langley Research Center
Hampton, Virginia 23665

Minimum Weight Design of Rectangular and Tapered Helicopter Rotor Blades with Frequency Constraints

by

Aditi Chattopadhyay*
Analytical Services & Materials, Inc.
Hampton, Virginia 23666
and
Joanne L. Walsh**
NASA Langley Reseach Center
Hampton, Virginia 23665

Abstract

The minimum weight design of a helicopter rotor blade subject to constraints on coupled flap-lag natural frequencies has been studied in this paper. A constraint has also been imposed on the minimum value of the autorotational inertia of the blade in order to ensure that the blade has sufficient inertia to autorotate in case of an engine failure. The program CAMRAD has been used for the blade modal analysis and the program CONMIN has been used for the optimization. In addition, a linear approximation analysis involving Taylor series expansion has been used to reduce the analysis effort. The procedure contains a sensitivity analysis which consists of analytical derivatives of the objective function and the autorotational inertia constraint and central finite difference derivatives of the frequency constraints. Optimum designs have been obtained for both rectangular and tapered blades. Design variables include taper ratio, segment weights, and box beam dimensions. The paper shows that even when starting with an acceptable baseline design, a significant amount of weight reduction is possible while satisfying all the constraints for both rectangular and tapered blades.

Nomenclature

b	box beam width
c	chord
f_1	frequency of 1^{st} lead-lag dominated mode
f_2	frequency of 1^{st} flapping dominated mode
g	constraint function
h	box beam height
$h(z)$	box beam height variation along blade span
n	number of blades
r_j	distance from the root to the center of the j^{th} segment
t_1, t_2, t_3	box beam wall thicknesses
x, y, z	reference axes
x_c	box beam center of mass location
A	box beam cross sectional area
A.I.	autorotational inertia
E	Young's modulus
F	objective function
GJ	torsional stiffness
I_{b_x}, I_{b_y}	principal area moments of inertia of box beam about reference axes
I_{o_x}, I_{o_y}	principal area moments of inertia of nonstructural mass about reference axes
I_x, I_y	total principal area moments of inertia about reference axes
I_θ	mass polar moment of inertia
L_j	length of j^{th} segment
M_{b_x}, M_{b_y}	mass moments of inertia of box beam about reference axes
M_{o_x}, M_{o_y}	mass moments of inertia of nonstructural weight about the reference axes
M_x, M_y	total mass moments of inertia about the reference axes
N	total number of blade segments
NDV	number of design variables
R	blade radius
W	total blade weight
$W(\phi)$	blade weight as a function of design variable ϕ
W_b	box beam weight
W_o	total weight of nonstructural blade weight and lumped/tuning weights
α	prescribed autorotational inertia
$\Delta\phi$	design variable increment
λ_h	taper ratio in z direction
ϕ_i	i^{th} design variable
ρ_j	mass density of the j^{th} segment

Subscripts and Superscripts

r	root value
t	tip value
L	lower bound
U	upper bound
$\hat{}$	approximate value

---

* Research Scientist, Member AIAA, AHS
** Aerospace Engineer, Member AIAA, AHS

Introduction

Computer-based mathematical programming methods for optimum design of structures have been under rapid development during the last two decades. Using mathematical processes, engineering design synthesis problems can be posed as sequences of analysis problems combining engineering models with minimization techniques. An extensive amount of work has been done in developing such design optimization procedures over the past few years to bring the state of the art to a high level[1-5]. These methods can now be applied to optimum design of practical structures such as aircraft[1,2,5] and helicopters[3-5]. The present paper focuses on helicopter rotor blade design.

The helicopter rotor blade design process requires a merging of several disciplines, including dynamics, aerodynamics, structures, and acoustics. Two of the major criteria in rotor blade design have been low weight and low vibration. For a helicopter in forward flight, the nonuniform flow passing through the rotor causes oscillating airloads on the rotor blades. These loads in turn are translated into vibratory shear forces and bending moments at the hub. One important design technique is to separate the natural frequencies of the blade from the harmonics of the airloads to avoid resonance. Failure to consider frequency placement in the predesign stage of the design process could cause a significant increase in the final blade weight since it generally involves postdesign addition of nonstructural masses. In order to avoid such weight penalties it is desirable to design and fabricate a helicopter blade and appropriately place the natural frequencies at an early stage in the design process. This can be done by a proper tailoring of the blade mass and/or stiffness distribution. This tailoring is not an easy task because of the complicated modes of the blade due to the presence of several coupling effects[6]. One such coupling is due to coupling of flap, lag, and torsional motions through the pitch angle blade twist and off-set between the elastic and inertia axes. The inclusion of these coupling effects makes the optimum design process highly complex. In the past, the conventional design process was controlled mainly by the designer's experience and the use of trial and error methods. Today, one of the more promising approaches to the helicopter rotor design process is the application of optimization techniques.

Due to the importance of the problem, a considerable amount of work has been aimed at various aspects of rotor blade vibration reduction[5-12]. A significant amount of this work has been devoted to reducing vibration by controlling the vertical hub shears and moments[8-13]. In Ref. 9 Taylor described the use of modal shaping. The objective of his work is to reduce vibration levels by modifying the mass and stiffness distributions to modify "modal shaping parameters" which are functions of blade mass distributions and mode shapes. These modal shaping parameters have been sometimes interpreted as "ad hoc" optimality criteria[11,13]. In Ref. 10 Bennett described a method for reducing the vertical shear transferred from the rotor blade to the mast by combining conventional helicopter engineering analysis with a nonlinear programming algorithm. Friedmann[11] considered the problem of minimizing hub shears or hub vibratory rolling moments subject to aeroelastic and frequency constraints. An early attempt at optimum blade design for proper placement of natural frequencies with a constraint on autorotational inertia was due to Peters[12] where he started with a baseline blade design and attempted to refine the design by trying to find a mass and stiffness distribution to give the desired frequencies. Reference 13 addressed the problem of optimum design for a typical soft-in-plane hingeless rotor configuration for minimum weight using optimality criteria approach. The results in Ref. 13 indicate that application of optimization techniques lead to benefits in rotor blade design not only through substantial weight reduction but also a considerable amount of reduction in the vibratory hub shears and moments at the blade root. In Ref. 14, Peters addressed a problem of the optimum design of a rectangular blade for proper placement of frequencies. However, he did not use the blade weight as the objective function due to a difficulty in finding a feasible design. Rather, he started his design with an objective function involving measures of the closeness of frequencies to desirable frequencies. Currently at the NASA Langley Research Center, there is an effort to integrate several technical disciplines in rotorcraft design. The present paper is part of this effort and deals with the dynamics aspect of design. The scope of the present work is to find the optimum mass and stiffness distributions which minimize the weight of a rotor blade, rectangular or tapered, undergoing coupled flap-lag vibrations. Constraints are imposed on the natural frequencies and the autorotational inertia of the blade. The present paper uses the same baseline blade as Peters with weight as the objective function. A first investigation in the effect of taper of the structure on the optimum blade design has been made and a study on the effect of the prescribed autorotational inertia constraint on the blade weight has been conducted.

Problem Statement, Test Problem, and Solution

The purpose of the present work is to arrive at minimum weight designs of rotor blades subject to constraints on the blade natural frequencies and autorotational inertia. The designs begin with an existing adequate blade design which will be referred to hereafter as the "reference blade." One way of reducing the vibration level in the blade is to design it such that the blade natural frequencies are separated from the driving frequencies (n per rev frequencies, where n denotes the number of blades). Since the frequencies of interest of the reference blade were already away from these critical values, it was decided to design the optimum

blade for minimum weight while constraining the desired frequencies to be within close ranges (windows) of the corresponding reference blade frequencies. Another important factor in rotor blade design is the ability of the blade to autorotate. Therefore, it was decided that the optimum blade should have at least the same value of rotary inertia as that of the reference blade.

Since the reference blade (Ref. 14) is an articulated blade with a rigid hub, no distinction is made between collective or cyclic modes for flapping and in-plane motions. The blade has a rectangular planform, a pretwist and a root spring which limits torsional motion. The blade data shown in Figure 1 and Table 1 (from Ref. 14) has a box beam with unequal vertical wall thicknesses located inside the airfoil (Fig. 1a). It is assumed that only the box beam (Fig. 1b) contributes to the blade stiffness, i.e., contributions of the skin, honeycomb, etc. to the blade stiffness are negligible. The details of the box beam section property calculations are presented in the Appendix.

Optimization Problem Formulation

The optimization problem is to minimize the weight of the blade. The constraints are upper and lower limits (windows) on the frequencies of the first lead-lag dominated mode and the first flapping dominated mode along with a prescribed lower limit on the autorotational inertia of the blade. The design variables include box beam dimensions, magnitudes of nonstructural weights and taper ratio.

The weight of the blade, W, consists of two components as follows:

$$W = W_b + W_o \tag{1}$$

where W_b represents the structural weight of the box beam and W_o represents the nonstructural weight of the blade plus the weight of the tuning/lumped masses added to the blade. The blade is discretized into finite segments (Fig. 2) and the blade weight in discretized form is given below:

$$W = \sum_{j=1}^{N} \rho_j A_j L_j + \sum_{j=1}^{N} W_{o_j} \tag{2}$$

where N represents the total number of segments.

The autorotational inertia of the blade is calculated as follows

$$A.I. = \sum_{j=1}^{N} W_j r_j^2 \tag{3}$$

where W_j is the total weight and r_j is the distance from the root to the center of the j^{th} segment. The frequency associated with the first lead-lag dominated mode is denoted f_1 and the frequency associated with the first flapping dominated mode is denoted f_2. The optimization problem can now be mathematically formulated as follows:

$$\text{minimize } W(\phi)$$

where the weight W is given by equation (2) and ϕ denotes the vector of design variables subject to the normalized constraints

$$g_1(\phi) = \frac{f_1}{f_{1_U}} - 1 \leq 0 \tag{4}$$

$$g_2(\phi) = 1 - \frac{f_1}{f_{1_L}} \leq 0 \tag{5}$$

$$g_3(\phi) = \frac{f_2}{f_{2_U}} - 1 \leq 0 \tag{6}$$

$$g_4(\phi) = 1 - \frac{f_2}{f_{2_L}} \leq 0 \tag{7}$$

$$g_5(\phi) = -\frac{A.I.}{\alpha} + 1 \leq 0 \tag{8}$$

and side constraints

$$\phi_{i_L} \leq \phi \leq \phi_{i_U} \tag{9}$$

In equations (4) and (5) f_{1_U} and f_{1_L} denote the upper and lower bound respectively on frequency f_1 and in equations (6) and (7) f_{2_U} and f_{2_L} denote the upper and lower bound respectively on frequency f_2. In equation (8) α represents the minimum acceptable value of the autorotational inertia and in equation (9) ϕ_i denotes the i^{th} design variable. By convention a constraint is satisfied when $g_k(\phi) \leq 0$.

The design variables considered are summarized in Table 3 for ten finite segments (i.e., N = 10). Cases 1 and 2 refer to the rectangular blade and cases 3 and 4 refer to the tapered blade. In case 1 (thirty design variables) the design variables are the wall thicknesses t_{1_i}, t_{2_i}, and t_{3_i}, i=1,2,...,10 (Fig. 1b). In case 2 (forty design variables) the segment nonstructural weights, W_{o_i}, i=1,2,...,10 are the ten additional design variables. Minimum values are imposed on t_1, t_2, and t_3 to provide adequate strength since stresses due to applied loads are not calculated. For the segment weight W_{o_i}, the lower bound is the "minimum nonstructural segment weight" in Table 1. For the tapered blade two new design variables are included in addition to those used in the rectangular

blade. They are the blade taper λ_h in the z direction (Fig. 4) and the box beam outer dimension h (Fig. 1b). It is assumed that the box beam height h varies linearly along the blade span as shown in Fig. 5. In case 3 (twelve design variables), the design variables are h_r, λ_h, and W_{o_i}, i=1,2,...,10, where h_r is the box beam height at the blade root. In case 4 (forty-two design variables), an additional thirty design variables have been used and they are t_{1_i}, t_{2_i}, and t_{3_i}, i=1,2,...,10.

Analysis

The modal analysis portion of the program CAMRAD,[15] which uses a modified Galerkin approach[16], has been used. According to Ref. 17, this approach is the preferred method for computing mode shapes and frequencies of structures having large radial variations in bending stiffness.

The general purpose optimization program CONMIN[18] which uses the nonlinear programming method of feasible directions has been used for the optimization. In the search for the optimum vector of new design variables, CONMIN requires derivatives of the objective function and constraints. The user has the option of either allowing CONMIN to calculate derivatives by using forward differences, or by supplying those derivatives to CONMIN. In this paper, the latter approach has been used. Analytical expressions have been obtained for the derivatives of the objective function and the autorotational inertia constraint. A central difference scheme has been used for the derivatives of the frequency constraints. The initial attempt using forward differences gave highly inaccurate derivatives.

Approximate Reanalysis Technique - The optimization process generally requires many evaluations of the objective function and the constraints before an optimum design is obtained. The process therefore can be very expensive if exact analyses are made for each evaluation. However, as Miura in Ref. 3 observed the optimization process primarily uses analysis results to move in the direction of the optimum design; therefore, a full analysis is required only occasionally during the design process and at the end to check the final design. Thus, various approximation techniques can be used during the optimization process to reduce the analysis cost. In the present paper, the objective function and constraints are approximated using a piecewise linear analysis based on first order Taylor series expansions. The expansions provide the changes in the objective function and constraints in terms of changes in the design variables and the derivatives obtained at the previous iteration. Specifically, if the objective function F, the constraint g, and their respective derivatives are calculated for the design variable ϕ_k using an exact analysis, their values for an increment in the design variable $\Delta\phi_k$ are as follows:

$$\hat{F} = F + \sum_{k=1}^{NDV} \frac{\partial F}{\partial \phi} \Delta\phi_k \qquad (10)$$

and

$$\hat{g} = g + \sum_{k=1}^{NDV} \frac{\partial g}{\partial \phi_k} \Delta\phi_k \qquad (11)$$

where the quantities denoted (^) represent approximate values and NDV denotes the number of design variables. The assumption of linearity is valid over small increments in the design variable values and does not introduce large errors if the increments are small. A "move limit", defined as the maximum fractional change of each design variable value, has been imposed as upper and lower bounds on ϕ_k for each design variable. Errors which may be introduced by use of the piecewise linear approach are controlled with the use of these move limits. In past applications of this technique (e.g., Ref. 19) and in the present work a move limit of 0.1 has been found to be satisfactory and has been used for all calculations.

Implementation

A flow chart describing the optimization procedure is shown in Fig. 3. Steps in the procedure are as follows:

ITERATION SCHEME

Step	Operation
1.	Discretize the blade and initialize the design variables.
2.	Compute box beam properties and calculate autorotational inertia of the blade based on current set of design variables.
3.	Perform blade modal analysis (frequencies and mode shapes) using CAMRAD.
4.	Calculate the objective function (weight) and compute the constraints on frequency and autorotational inertia.
5.	Check for convergence of the objective function (a change within a convergence tolerance of 0.5×10^{-5} over three consecutive cycles). If not converged go to steps 6-8.
6.	Calculate the derivatives of frequency constraints. Perturb each design variable by $\Delta\phi_k$. Repeat steps 2 and 3 for $\phi_k+\Delta\phi_k$. Repeat steps 2 and 3 for $\phi_k-\Delta\phi_k$. Use central differences for the frequency derivatives. Evaluate analytical expressions for the autorotational inertia and the objective function derivatives.
7.	Update the design variables using CONMIN and approximate analysis.
8.	Repeat steps 2-7.

Results and Discussion

The blade has been discretized into ten segments along the span (Fig. 2) and details of the blade segment data are presented in Table 1. In Table 1 the entry "minimum nonstructural segment weight" represents the weight of the skin, honeycomb, etc. of a segment and "total nonstructural segment weight" denotes the weight of the skin, honeycomb, etc. along with the lumped/tuning weight of that segment. The rotor preassigned parameters (the parameters that remain fixed during the optimization process) are presented in Table 2. A modal analyses of the reference blade has been performed and the frequencies of the first lead-lag dominated mode (f_1) and the first flapping dominated mode (f_2) have been used to set up the frequency windows. The windows are ±1 percent of these calculated values. Results are presented for a rectangular as well as a tapered blade with various combinations of design variables. Several local minima have been found and the best of these results are presented here. The effect of different starting points on optimum results has been investigated and is discussed later.

Rectangular Blade

The first part of the study considers a rectangular blade with a rectangular box beam (Fig. 1b). The results for cases 1 and 2 are presented in Table 4. Typically ten to fifteen cycles have been necessary to arrive at optimum designs. From Table 4 the frequency f_1 (lead-lag dominated) is at its upper bound after optimization and the autorotational inertia constraint is active, i.e., the value is equal to the prescribed value, in all cases. The weight reductions from the reference to the optimum blade configurations have been between 8.5 percent and 13.2 percent which are substantial. Figs. 6-12 depict the optimum versus the reference blade design variable distributions along the blade span. Figures 6-8 show the optimum versus the reference blade design variable distributions for the thirty design variable case (case 1). Figures 6 and 7 demonstrate that the optimization process reduces the wall thicknesses t_1 and t_2 (Fig. 1b) inboard and increases them outboard. Figure 6 shows that the wall thickness t_3 (Fig. 1b) is increased in each segment by the optimization process. Figures 9-12 represent the optimum versus the reference blade design variable distributions for the forty design variable case (case 2). Figures 9 and 10 demonstrate a significant redistribution of the wall thicknesses t_1 and t_2 with increase at the blade tip. The vertical wall thickness t_3 is increased by the optimization process as shown in Fig. 11 and the trend is similar to that of case 1 (Fig. 8). A significant reduction in the segment nonstructural weight distribution is apparent from Fig. 12 with the lowest value toward the blade root. Overall, the optimum distributions (cases 1 and 2) demonstrate an increase in blade weight towards the tip which is caused by the inclusion of the autorotational inertia constraint which requires larger masses outboard.

Tapered Blade

The second part of the study considers a blade where the taper ratio has been allowed to be a design variable during optimization. In essence, a change in the blade planform has been allowed which would mean a change in the blade aerodynamic performance. In other words, instead of starting from an aerodynamic design and modifying the structural parameters for better dynamic performance, a new design of the blade has been addressed from the minimum weight and dynamics performance point of view. The associated optimum design problem can no longer be termed as a redesign process.

In order to maintain the airfoil height to chord ratio fixed, the h/b ratio has been held constant throughout the blade span during the optimization process. A value of h/b = 0.25 has been used which corresponds to the reference blade value.

Optimum results have been obtained within eight to ten cycles. The results are summarized in Table 5. It is interesting to note from Table 5 that the weight reduction increases from 1.7 percent in the twelve design variable case (case 3) to 14.3 percent in the forty-two design variable case (case 4). Also the taper ratio changes from a high value of 2.44 in case 3 to a more realistic value of 1.11 in case 4. The optimum versus the reference blade design variable distributions are shown in Figs. 13-17. Figure 13 shows the segment nonstructural weight distribution before and after optimization for case 3 (twelve design variables). The optimization process redistributes the weights, with a minimum value at the third and the fourth segment. The minimum value indicates that no additional lumped weights are necessary at those two segments. Figures 14-16 show significant redistributions of the wall thickness distributions after optimization for the forty-two design variable case. The trends are similar to that of the rectangular blade. The optimization process reduces the nonstructural segment weight as shown in Fig. 17, however, the values at each segment are higher than the corresponding lower bounds indicating the necessity of lumped weights at each segment.

Autorotational Inertia Study

A study has been conducted on the sensitivity of the optimum design variables and objective function to changes in the value of the prescribed autorotational inertia. The results of this study for a rectangular blade with forty design variables (case 2) are presented in Table 6 where the increments in the prescribed autorotational inertia are ±5 percent of the nominal value (517.3 lb-in^2). The results indicate that increases in the magnitude of the prescribed rotary inertia value increases the weight of the optimum blade. For example, a 5 percent increase in the rotary inertia value produces a 13.3 percent increase in the optimum blade weight.

Some typical changes in the design variable distributions are shown in Figs. 18 and 19.

Observations on the Optimization Process

Since optimum design problems are prone to the existence of local minima, several sets of starting designs have been used. Depending upon the initial design, alternate optimum designs have been obtained. For instance, for the rectangular blade with thirty design variables (case 1), the percentage weight reduction increased from 6.3 to 8.5 with a change in the starting design (Table 7). For the case of the tapered blade there is also a significant change in the blade weight reduction with change in initial design (Table 8). Also the optimum value of the taper ratio λ_h changes considerably with the change in initial design. Hence, it is worthwhile investigating different starting designs to obtain the better of the alternate designs from among the several relative optima. In addition to trying several alternate starting designs, attempts have also been made at improving the optimum designs by scaling design variables and changing several CONMIN control parameters. No significant improvement has been noticed by scaling the design variables. Change of certain control parameters in CONMIN (such as step sizes and/or tolerances) improves the optimum results.

Concluding Remarks

In this paper, the minimum weight design of a helicopter rotor blade with constraints on coupled flap-lag natural frequencies has been studied. A minimum value constraint on the autorotational inertia of the blade has also been imposed in order to ensure sufficient rotary inertia for the blade to autorotate. The program CAMRAD has been used to perform blade modal analysis and the program CONMIN has been used for the optimization. In addition, a linear approximation technique involving Taylor series expansion has been used. A sensitivity analysis consisting of analytical expressions for the derivatives of the objective function and the autorotational inertia constraint and central difference derivatives of the frequency constraints has been performed. Optimum design have been obtained for blades with both rectangular and tapered planforms. The design variables used are the box beam dimensions, taper ratio and segment weights.

The following conclusions have been drawn from the present study. In the frequency derivative calculations use of forward difference scheme led to numerical difficulties which have been overcome by the use of central differences. The optimization program CONMIN along with the linear approximations based on Taylor series expansion has been very efficient and is typically able to arrive at an optimum design in eight to fifteen cycles. The results of the optimization clearly indicate a significant amount of weight reduction from the reference to the optimum blade while satisfying all the imposed constraints. The optimum design variable distributions indicate a tendency of introducing larger wall thicknesses towards the tip of the blade. This is due to the presence of the autorotational inertia constraint which increases in magnitude with the increase in the moment arm. Results of a study on the effect of prescribed autorotational inertia indicate a large effect on the optimum blade weight as well as the design variable distribution. For example, a 5 percent increase in the prescribed autorotational inertia value (from the nominal value) increases the optimum blade weight by 13.3 percent. Therefore the study provides data for a trade-off study between autorotational inertia and weight. Finally due to the existence of several local minima, starting the optimum design process with different initial sets of the design variables has been found to produce better optima.

Appendix

Sectional Properties

A typical rotor blade section with a nonuniform box beam is shown in Fig. 1. It is assumed that the structural stiffness is contributed by the box beam with unequal wall thicknesses and that the beam material is linearly elastic. The effects of shear deformation due to transverse forces and the effects of rotary inertia are assumed to be negligible, however shear due to torsion is considered. The overall cross sectional properties are calculated as follows:

$$W = W_b + W_o \tag{1}$$

$$I_x = I_{b_x} + I_{o_x} \tag{2}$$

$$I_y = I_{b_y} + I_{o_y} \tag{3}$$

$$M_x = M_{b_x} + M_{b_x} \tag{4}$$

$$M_y = M_{b_y} + M_{o_y} \tag{5}$$

and

$$I_\theta = M_x + M_y \tag{6}$$

The quantities with subscript 'b' denotes the box beam contributions and subscript 'o' refers to the contributions from the remainder of the blade section.

Box Beam Properties

The cross sectional area is given as (Fig. 1)

$$A = bh - \bar{b}\bar{h} \tag{7}$$

where

$$\bar{b} = b - (t_2 + t_3)$$

and

$$\bar{h} = h - 2t_1$$

The location of the center of mass is given by

$$x_c = \frac{\frac{b^2}{2}h - \frac{\bar{b}^2}{2}\bar{h} - \bar{b}\bar{h}t_2}{A} \tag{8}$$

The expressions for the area moments of inertia are

$$I_{b_x} = \frac{bh^3}{12} - \frac{\bar{b}\bar{h}^3}{12} \tag{9}$$

and

$$I_{b_y} = \frac{b^3h}{12} - \frac{\bar{b}^3\bar{h}}{12} + bh\left(\frac{b}{2} - x_c\right)^2 + bh\left(\frac{b}{2} - x_c\right)^2 - \bar{b}\bar{h}\left(\frac{\bar{b}}{2} + t_2 - x_c\right)^2 \tag{10}$$

The mass moments of inertia of the box beam with respect to flapping and inplane, M_{b_x} and M_{b_y} respectively, are calculated as follows:

$$M_{b_x} = \rho I_{b_x} \tag{11}$$

$$M_{b_y} = \rho I_{b_y} \tag{12}$$

where ρ denotes the density of the box beam material. The calculation for the torsional rigidity is explained in detail in References 14 and 20.

References

1. Ashley, H., "On Making Things the Best - Aeronautical Use of Optimization," AIAA J. Aircraft 19, No. 1, 1982.

2. Sobieszczanski-Sobieski, J., "Structural Optimization Challenges and Opportunities," presented at Int. Conference on Modern Vehicle Design Analysis, London, England, June 1983.

3. Miura, H., "Application of Numerical Optimization Method to Helicopter Design Problems: A Survey," NASA TM 86010, October 1984.

4. Bennett, R. L., "Application of Optimization Methods to Rotor Design Problems," Vertica, Vol. 7, No. 3, 1983, pp. 201-208.

5. Sobieszczanski-Sobieski, Jaroslaw, "Recent Experiences in Multidisciplinary Analysis and Optimization," NASA CP 2327, 1984.

6. Peters, D. A., Ko, Timothy, Rossow, Mark P., "Design of Helicopter Rotor Blades for Desired Placement of Natural Frequencies," Proc. of the 39th Annual Forum of the AHS, May 9-11, 1983, St. Louis, Missouri.

7. Reichert, G., "Helicopter Vibration Control - A Survey," Vertica, Vol. 5, 1981, pp. 1- 20.

8. Friedmann, P. P., "Response Studies of Rotors and Rotor Blades with Application to Aeroelastic Tailoring," Semi-Annual Progress Report on Grant NSG-1578, December 1981.

9. Taylor, R. B., "Helicopter Vibration Reduction by Rotor Blade Modal Shaping, "Proc. of the 38th Annual Forum of the AHS, May 4-7, 1982, Anaheim, California.

10. Bennett, R. L., "Optimum Structural Design," Proc. of the 38th Annual Forum of the AHS, May 4-7, 1982, Anaheim, California, pp. 90-101.

11. Friedmann, P. P. and Shantakumaran, P., "Optimum Design of Rotor Blades for Vibration Reduction in Forward Flight," Proc. of the 39th Annual Forum of the AHS, May 9-11, St. Louis, Missouri.

12. Peters, D. A., "Design of Helicopter Rotor Blades for Optimum Dynamic Characteristics," Progress Report on Grant NAG-1-250, January 1985.

13. Hanagud, S., Chattopadhyay, Aditi, Yillikci, Y. K., Schrage, D., and Reichert, G., "Optimum Design of a Helicopter Rotor Blade," presented at the 12th European Rotorcraft Forum, Garmisch-Partenkirchen, West Germany, September 22-25, 1986, p. 26.

14. Peters, D. A., Ko, Timothy, Korn, Alfred, and Rossow, Mark P., "Design of Helicopter Rotor Blades for Optimum Dynamic Characteristics," Progress Reports, NASA Research Grant Number NAG-1-250, January 1982 through January 1985.

15. Johnson, W., "A Comprehensive Analytical Model of Rotorcraft Aerodynamics and Dynamics," Part II: User's Manual, NASA TM 81193, June 1980.

16. Lang, K. W., and Nemat-Nasser, S., "An Approach for Estimating Vibration Characteristics of Nonuniform Rotor Blades," AIAA Journal, Vol. 17, No. 9, September 1979.

17. Johnson, W., "A Comprehensive Analytical Model of Rotorcraft Aerodynamics and Dynamics," Part I: Analysis Development, NASA TM 81182, June 1980.

18. Vanderplaats, G. N., "CONMIN - A Fortran Program for Constrained Function Minimization," User's Manual, NASA TMX-62282, August 1973.

19. Walsh, Joanne L., "Applications of Numerical Optimization Procedures to a Structural Model of a Large Finite-Element Wing," NASA TM 87597, 1986.

20. Chattopadhyay, Aditi, "Optimization of Vibrating Beams Including the Effects of Coupled Bending and Torsional Modes," Ph.D. Thesis, Georgia Institute of Technology, June 1984.

Table 1. Reference blade data (Figs. 1 and 2)

Box beam height 'h' = 0.117 ft
Box beam density 'ρ' = 8.645 slugs/ft^3
Box beam width 'b' = 0.463 ft
Young's modulus 'E' = 2.304 x 10^9 lb/ft^2

Segment Number	Length (ft)	Box beam dimension (ft)			Bending stiffness x 10^4 (lb - ft^2)		Torsional stiffness x 10^4 (lb-ft^2)	Nonstructural segment weight (lbs) W_o		Pretwist (deg.)
	L	t_1	t_2	t_3	EI_x	EI_y	GJ	Total	Min.	
1	1.37	0.0116	0.0080	0.0280	7.349	78.58	11.111	6.718	0.89	1.745
2	2.2	0.0100	0.0100	0.0440	6.957	84.68	10.139	9.088	1.435	2.617
3	2.2	0.0075	0.0075	0.0325	5.548	66.55	7.778	1.978	1.435	5.594
4	2.2	0.0060	0.0050	0.0050	4.128	35.40	5.833	1.435	1.435	8.725
5	2.2	0.0050	0.0050	0.0045	3.537	31.20	5.000	2.352	1.435	6.805
6	2.2	0.0050	0.0050	0.0035	3.514	29.89	4.861	5.852	1.435	5.235
7	2.2	0.0050	0.0050	0.0040	3.526	30.55	4.931	6.342	1.435	3.49
8	2.2	0.0050	0.0050	0.0046	3.539	31.31	5.000	6.573	1.435	0.00
9	2.2	0.0050	0.0050	0.0035	3.514	29.89	4.861	6.372	1.435	-0.175
10	2.2	0.0050	0.0050	0.0021	3.481	27.91	2.778	5.962	1.435	-1.915

Table 2. Blade preassigned properties

Number of blades	4
Blade radius	22 ft
Chord	1.3 ft
Flap hinge offset	0.833 ft
Inplane hinge offset	0.833 ft
Solidity (based on mean chord)	0.0748
Precone angle	0 degree
Droop angle	0 degree
Tip sweep	0 degree
Pitch axis droop	0 degree
Pitch axis sweep	0 degree
Rotor speed	293 rpm

Table 3. Summary of design variables for cases studied

Case	Number of design variables	Planform	Design variables[a]
1	30	Rectangular	$t_{1_i}, t_{2_i}, t_{3_i}$
2	40	Rectangular	$t_{1_i}, t_{2_i}, t_{3_i}, W_{o_i}$
3	12	Tapered	h_r, λ_h, W_{o_i}
4	42	Tapered	$h_r, \lambda_h, t_{1_i}, t_{2_i}, t_{3_i}, W_{o_i}$

a - i=1,2,...,10

Table 4. Optimization results for rectangular box beam;
f_{1_L}=12.162 Hz, f_{1_U}=12.408 Hz,
f_{2_L}=15.936 Hz, f_{2_U}=16.258 Hz

	Reference blade	Optimum blade Case 1	Case 2
f_1 (hz)	12.285	12.408	12.408
f_2 (Hz)	16.098	15.945	15.94
Autorotational inertia (lb-ft^2)	517.3	517.3	517.3
Blade weight (lb)	98.27	89.92	85.27
Percent reduction in blade weight[a]	-	8.506	13.230

a - From reference blade

Table 5. Optimization results for tapered box beam;
f_{1_L}=12.162 Hz, f_{1_U}=12.408 Hz,
f_{2_L}=15.936 Hz, f_{2_U}=16.258 Hz

	Reference blade	Optimum blade Case 3	Case 4
λ_h	1.0	2.44	1.111
f_1 (Hz)	12.285	12.405	12.225
f_2 (Hz)	16.098	15.99	15.822
Autorotational inertia (lb-ft^2)	517.3	517.3	517.3
Blade weight (lb)	98.27	96.63	84.24
Percent reduction in blade weight[a]	-	1.67	14.28

a - From Reference Blade

Table 6. Sensitivity of optimum design with respect to prescribed autorotational inertia for Case 2 - rectangular blade

Prescribed A.I. value ($lb\text{-}ft^2$)	Increment[a] in A.I. value (%)	Optimum blade weight (lb) (lb)	Weight change from nominal (%)
465.6	-10	75.69	-11.23
504.4	-5	80.42	-5.69
517.3	0	85.27	0
543.2	5	96.63	13.32
569.0	10	96.76	13.48
594.9	15	98.21	15.17
620.8	20	102.44	20.13

a - Relative to nominal value.

Table 7. Effect of initial design on optimum results for the case 1, rectangular blade; f_{1_L}=12.162 Hz, f_{1_U}=12.408 Hz, f_{2_L}=15.936 Hz, f_{2_U}=16.258 Hz

	Reference blade	Optimum blade[a]	Optimum blade[a]
f_1 (Hz)	12.285	12.406	12.408
f_2 (Hz)	16.098	15.947	15.945
Autorotational inertia ($lb\text{-}ft^2$)	517.3	517.3	517.3
Blade weight (lb)	98.27	92.06	89.92
Percent reduction in blade weight	-	6.320	8.506

a - Refer to two alternate optimum designs with two different initial designs

Table 8. Effect of initial design on optimum results for case 4, tapered blade; f_{1_L}=12.162 Hz, f_{1_U}=12.408 Hz, f_{2_L}=15.936 Hz, f_{2_U}=16.258 Hz

	Reference blade	Optimum blade[a]	Optimum blade[a]
λ_h	1.0	2.387	1.111
f_1 (Hz)	12.285	12.409	12.225
f_2 (Hz)	16.098	15.94	15.822
Autorotational inertia ($lb\text{-}ft^2$)	517.3	518.4	517.3
Blade weight (lb)	98.27	95.25	84.24
Percent reduction in blade weight	-	3.07	14.28

a - Refers to two alternate optimum designs with two different initial designs

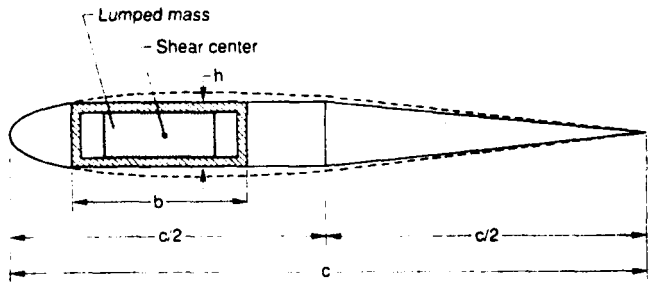

a) Airfoil cross section

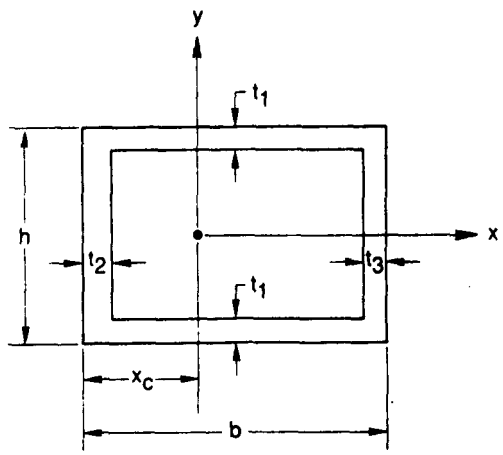

b) Box beam cross section

Fig. 1 Rotor blade cross section

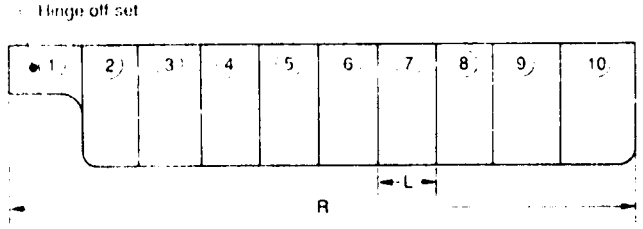

Fig. 2 Discretized rotor planform

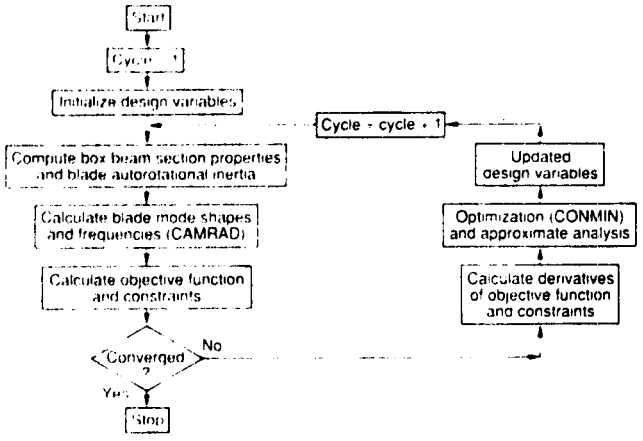

Fig. 3 Flowchart of the optimization process

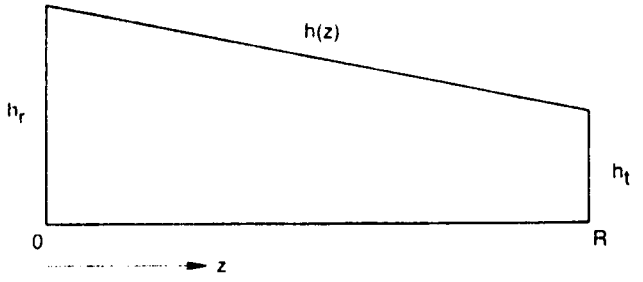

$$h(z) = h_r(1-z/R) + h_t\, z/R$$

Fig. 4 Rotor blade taper

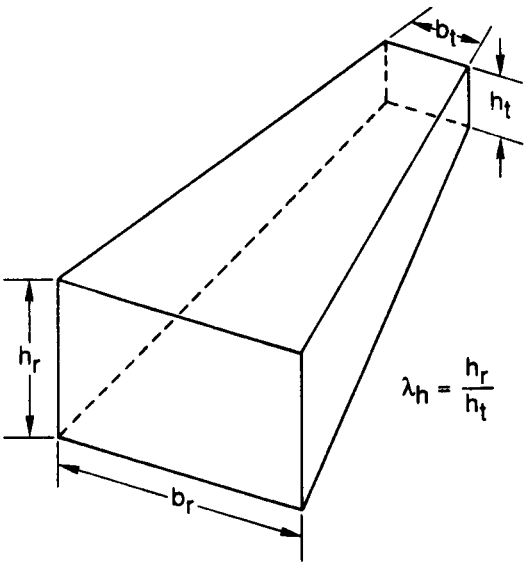

Fig. 5 Tapered box beam

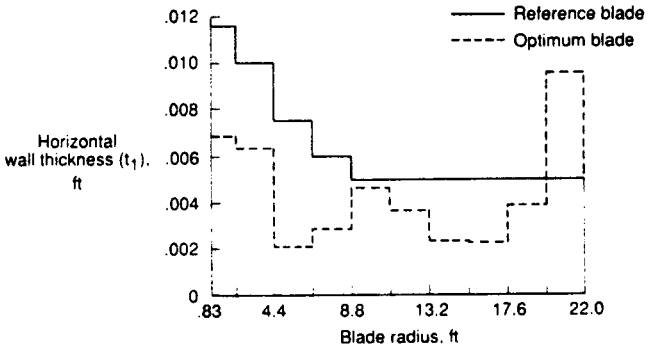

Fig. 6 Optimum versus reference blade t_1 distribution along blade span, case 1 (30 design variables, rectangular)

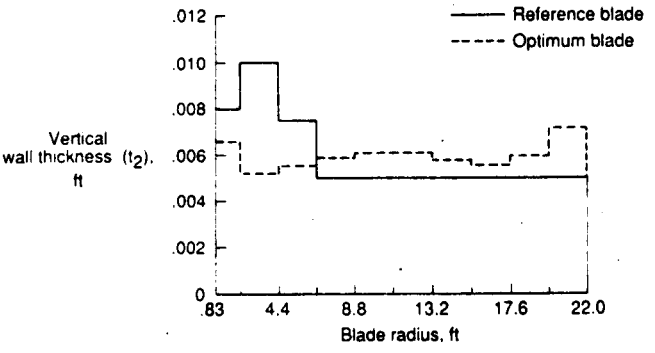

Fig. 7 Optimum versus reference blade t_2 distribution along blade span, case 1 (30 design variables, rectangular)

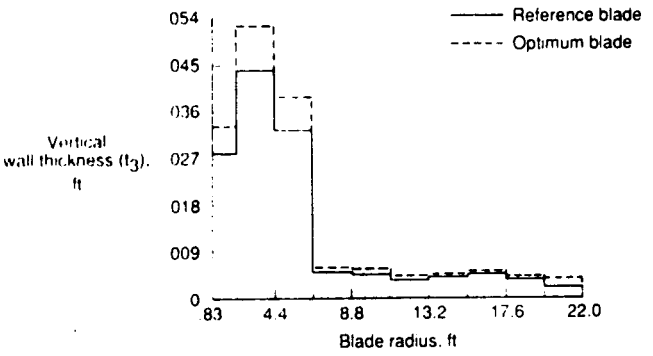

Fig. 8 Optimum versus reference blade t_3 distribution along blade span, case 1 (30 design variables, rectangular)

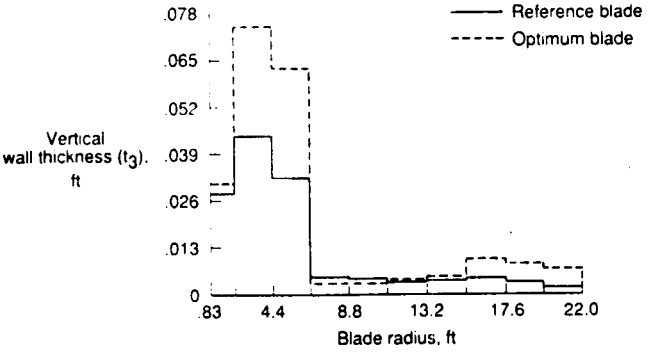

Fig. 11 Optimum versus reference blade t_3 distribution along blade span, case 2 (40 design variables, rectangular)

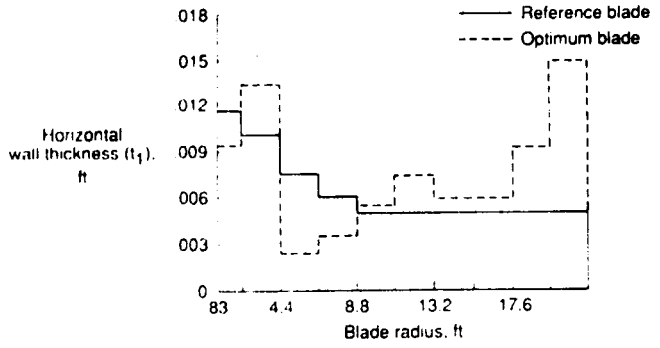

Fig. 9 Optimum versus reference blade t_1 distribution along blade span, case 2 (40 design variables, rectangular)

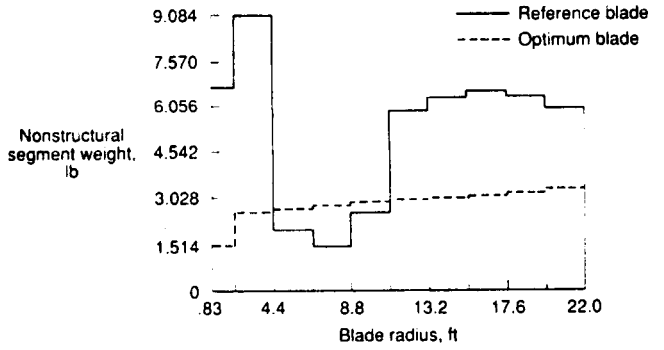

Fig. 12 Optimum versus reference blade segment mass distribution along blade span, case 2(40 design variables, rectangular)

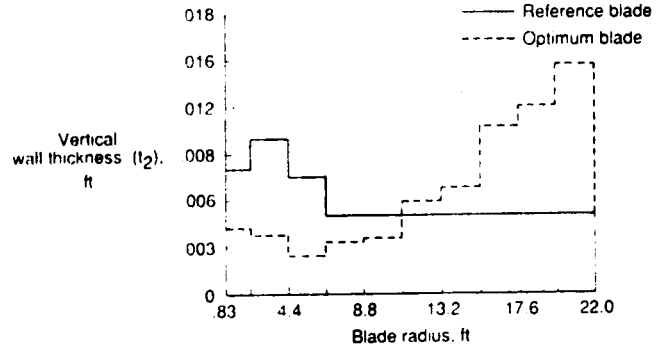

Fig. 10 Optimum versus reference blade t_2 distribution along blade span, case 2 (40 design variables, rectangular)

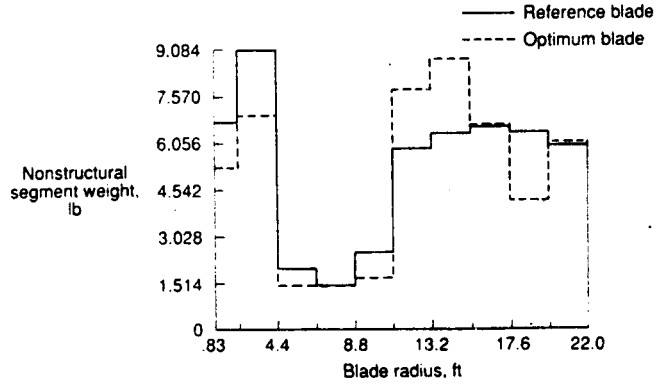

Fig. 13 Optimum versus reference blade segment mass distribution along blade span, case 3 (12 design variables, tapered)

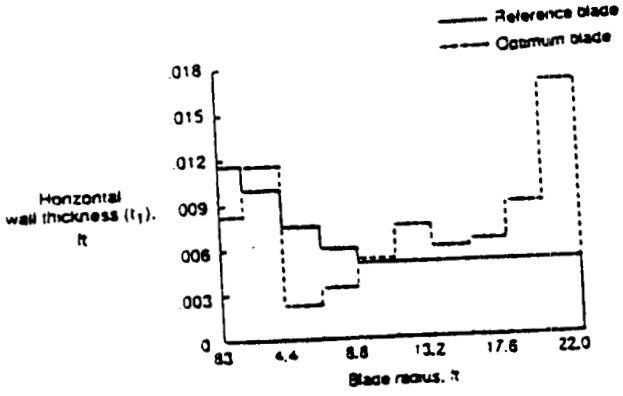

Fig. 14 Optimum versus reference blade t_1 distribution along blade span, case 4 (42 design variables, tapered)

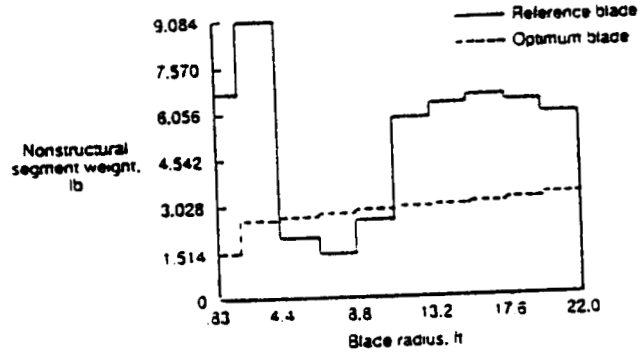

Fig. 17 Optimum versus reference blade segment mass distribution along blade span, case 4 (42 design variables, tapered)

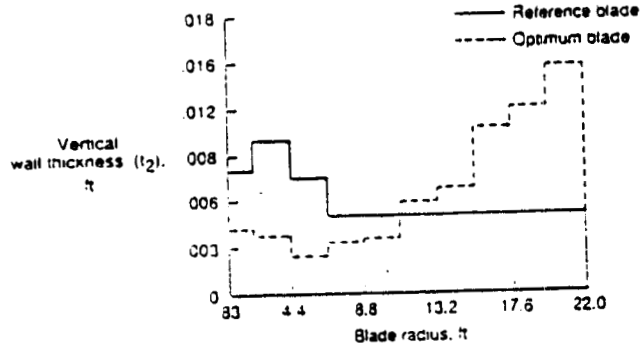

Fig. 15 Optimum versus reference blade t_2 distribution along blade span, case 4 (42 design variables, tapered)

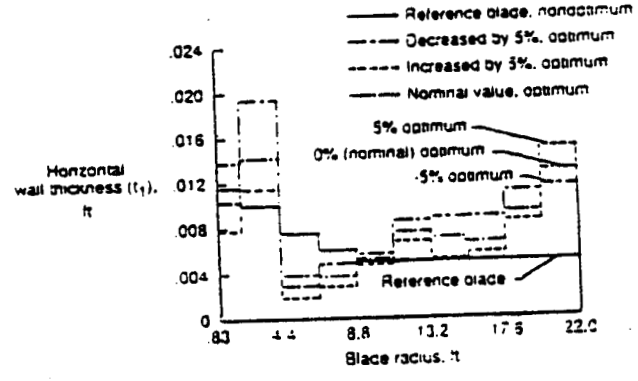

Fig. 18 Sensitivity of optimum wall thickness distribution (t_1) to changes in prescribed rotary inertia, case 2 (40 design variables, rectangular)

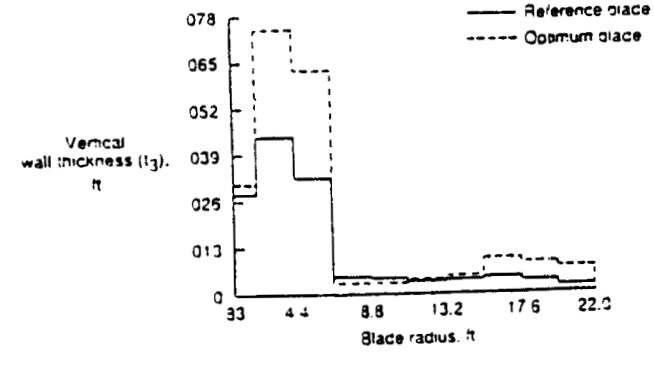

Fig. 16 Optimum versus reference blade t_3 distribution along blade span, case 4 (42 design variables, tapered)

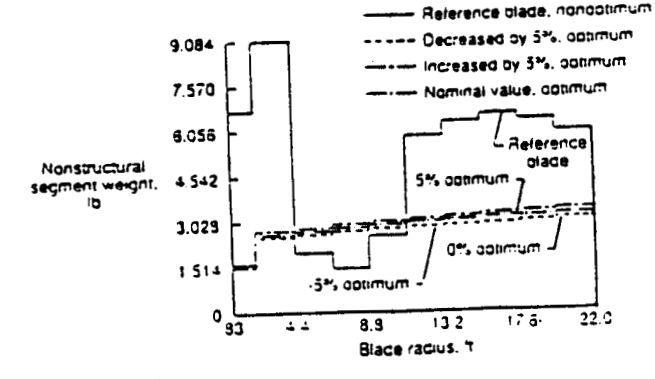

Fig. 19 Sensitivity of optimum nonstructural weight distribution to changes in prescribed rotary inertia, case 2 (40 design variables, rectangular)

NASA

Report Documentation Page

1. Report No.	2. Government Accession No.	3. Recipient's Catalog No.
NASA TM-100561		

4. Title and Subtitle

Minimum Weight Design of Rectangular and Tapered Helicopter Rotor Blades with Frequency Constraints

5. Report Date

February 1988

6. Performing Organization Code

7. Author(s)

Aditi Chattopadhyay and Joanne L. Walsh

8. Performing Organization Report No.

10. Work Unit No.

505-61-51

9. Performing Organization Name and Address

NASA Langley Research Center
Hampton, VA 23665-5225

11. Contract or Grant No.

13. Type of Report and Period Covered

Technical Memorandum

12. Sponsoring Agency Name and Address

National Aeronautics and Space Administration
Washington, DC 20546

14. Sponsoring Agency Code

15. Supplementary Notes

Paper to be presented at the 2nd International Conference on Rotorcraft Basic Research, College Park, MD, February 16-18, 1988.

16. Abstract

The minimum weight design of a helicopter rotor blade subject to constraints on coupled flap-lag natural frequencies has been studied in this paper. A constraint has also been imposed on the minimum value of the autorotational inertia of the blade in order to ensure that the blade has sufficient inertia to autorotate in case of an engine failure. The program CAMRAD has been used for the blade modal analysis and the program CONMIN has been used for the optimization. In addition, a linear approximation analysis involving Taylor series expansion has been used to reduce the analysis effort. The procedure contains a sensitivity analysis which consists of analytical derivatives of the objective function and the autorotational inertia constraint and central finite difference derivatives of the frequency constraints. Optimum designs have been obtained for both rectangular and tapered blades. Design variables include taper ratio, segment weights, and box beam dimensions. The paper shows that even when starting with an acceptable baseline design, a significant amount of weight reduction is possible while satisfying all the constraints for both rectangular and tapered blades.

17. Key Words (Suggested by Author(s))	18. Distribution Statement
Helicopter, minimum weight, frequencies, optimization, CAMRAD, CONMIN, autorotational inertia	Unclassified - Unlimited Subject Category 05

19. Security Classif. (of this report)	20. Security Classif. (of this page)	21. No. of pages	22. Price
UNCLASSIFIED	UNCLASSIFIED	14	A02